



Invited Review

Tectonics vs eustasy: The oceanic container and its contents

Bilal U. Haq^{a,b,*}, Sierd Cloetingh^c^a Sorbonne University, Paris, France^b George Mason University, Fairfax, VA, USA^c Utrecht University, Utrecht, the Netherlands

ARTICLE INFO

Keywords:

Eustasy and geodynamics

Long and short-term drivers of sea-level change

Hypsometry and sea-level change

Deep water cycling and sea-level change

ABSTRACT

Sea-level change over Earth's history reflects the interplay of water volume and the ever-shifting architecture of ocean basins. While short-term fluctuations (10^3 – 10^5 yr) often trace the advance and retreat of glaciers and ice caps, multi-million-year trends (10^7 – 10^9 yr) arise from deep-Earth processes – seafloor spreading, subduction, intraplate deformation, mantle plume upwelling, and the emplacement of large igneous provinces – that remodel basin volume and modulate the ocean's water budget. New geodynamic models now discard the assumption of steady-state mantle regassing and degassing, showing instead that persistent imbalances can lock water into the interior or release it back to the surface, sculpting long-term sea-level trajectories.

Recent advances in seismic and tomographic imaging, coupled with high-resolution numerical simulations, have fostered an emerging convergence between geodynamic theory and stratigraphic records of Phanerozoic sea-level curves – particularly for second-order (multi-million years) Meso-Cenozoic variations. These efforts also cast doubt on earlier reconstructions based solely on continental flooding metrics without accounting for evolving hypsometries. Superimposed on these tectonic signals are third-order cycles driven largely by Earth's orbital rhythms: long-period Milankovitch modulations (~ 1.2 Myr obliquity, especially common during re-frigerations, and ~ 2.4 Myr eccentricity, recurrent during warm intervals) leave clear imprints in sequence stratigraphic, deep-sea hiatuses, fossil diversity patterns, and stable-isotopic records. Meanwhile, the capacity of small, hydrous mantle plumes to shuttle water across the core-mantle boundary – and the topographic uplift associated with flood basalt provinces – emerges as an underappreciated influence on regional sea-level anomalies. Despite these advances, reconstructing pre-Cretaceous sea-level history remains hampered by scant constraints on ancient spreading and subduction systems. Addressing these gaps and achieving further advancements demands enhanced temporal resolution and more complete datasets – especially for younger intervals where the oceanic lithosphere is preserved with greater fidelity. Seismic and tomographic surveys in under-sampled regions, such as Africa, South America and West Antarctica, are especially critical. Legacy industry data could help fill key gaps, and broader access to publicly funded datasets is vital. Sea-level change stands as one of the most societally-relevant challenges in geoscience and meeting its demands will require sustained investment in advanced data collection, robust modeling, and collaborative partnerships between academia and industry.

Contents

1. Introduction and scope	1
2. Mesozoic land- and sea-scapes	3
2.1. Paleogeographic and paleo-kinematic approaches	3
2.2. Hypsometric considerations	4
2.3. Seafloor production rates	4
2.4. Mantle-lithosphere dynamics and its impact on surface topography	5
2.5. The role of plumes	5

* Corresponding author at: Sorbonne University, Paris, France.

E-mail address: bilhaq@gmail.com (B.U. Haq).<https://doi.org/10.1016/j.earscirev.2025.105166>

Received 6 March 2025; Received in revised form 8 May 2025; Accepted 12 May 2025

Available online 15 May 2025

0012-8252/© 2025 The Authors. Published by Elsevier B.V. This is an open access article under the CC BY license (<http://creativecommons.org/licenses/by/4.0/>).

2.6. Large igneous province emplacements	5
3. Deep-water recycling through the mantle	6
4. Glacio-eustasy	7
5. Long and short-term variations of sea level	7
5.1. Mesozoic sea-level variations (updated)	8
5.2. Third-order and higher-frequency cycles	8
6. Discussion and outlook	9
Declaration of competing interest	10
Acknowledgements	10
Data availability	10
References	10

1. Introduction and scope

In a thought-provoking article on Cretaceous eustasy, marine geologist Seymour Schlanger (1986) reviewed the mechanisms of high-frequency sea-level change (SLC) and concluded that the global causes of these variations cannot be fully understood through stratigraphy alone and that the solution may ultimately require geophysical input. This insight, though perhaps not as prescient today, was a critical step in the evolution of SLC research. Over time, both stratigraphers and geophysicists have made significant strides in understanding SLC, though their research interests have often diverged. Geodynamicists (with some exceptions, e.g., Cloetingh et al., 1985) have primarily focused on mechanisms driving SLC on longer timescales (many millions of years), while stratigraphers have concentrated on resolving sedimentary cycles on shorter timescales, typically modulated by long-term Milankovitch periodicities, which are generally less than 2.5 million years (Myr).

The interactions between tectonic and climatic processes highlight the dual nature of sea-level (SL) controls – surface processes that alter volume and deep Earth processes that modify basin geometry and thus the ocean's water holding capacity. On the shorter scales, global (eustatic) SLCs and their potential drivers are now relatively better understood along with explanations for local anomalies in amplitude measurements – as the discussion and citations later in this review will attest. Nevertheless, the causes of long-term SLC are complex, operating on vastly different timescales and with varied impacts. Given that the stratigraphic record integrates both eustatic and eurybatic (regional) signals, untangling the contributions of each becomes increasingly difficult as we delve further back in deeper time. Despite these challenges, research in this area has accelerated in recent years, which is the subject of this paper.

A decade ago, we examined the growing body of evidence linking solid-Earth geodynamics to the soft-rock record of SLC (Cloetingh and

Haq, 2015) and noted the increasing collaboration across disciplines in SL research. Since then, several groups have explored the interconnections among tectonics, climate, and SLCs, with a particular focus on the Mesozoic Era, which spans the initiation of Pangean breakup and the ongoing cycle of continental collisions. Conrad (2013) provided a valuable review that highlighted the multiple timescales of solid-Earth processes, both short and long, that can affect both eurybatic and eustatic SLCs, and Young et al.'s (2022) more recent modeling study updates some of the long-term factors and amplitudes of SLC associated with them. Another perspective is provided by Simmons et al. (2020), whose review outlines some of the general contributing processes to long- and short-term SL variations, primarily through the lens of stratigraphic analysis.

Conrad (2013) categorized fast-acting processes, such as elastic isostatic response to ice and water loading/unloading during glaciations and deglaciations (timescales of 10^1 – 10^2 years), followed by slower processes like viscous post-glacial flow (timescales of 10^3 – 10^5 years). While these processes do not drive global SLCs, they generate regional eurybatic anomalies. He argued that variations in SL due to climate-induced factors, such as glaciation and water temperature changes, that exceed 57 m (64 m when compensated for isostatic response) are more likely to be caused by changes in ocean basin volume. A key driver of oceanic volume changes on these timescales is sediment input. Using sediment thickness data and the area-age distribution of Müller et al. (2008), he estimated a SL rise of ~60 m in the Cenozoic due to new sediment flux into the ocean margins. Fraught with significant uncertainties, these estimates, nevertheless, provide first-order constraints on the contributions of various drivers (Fig. 1).

Mantle-driven dynamic topography (DT) can also influence global SL by altering seafloor bathymetry, which in turn affects the volumetric capacity of ocean basins. One model-based estimate (Spasojević and Gurnis, 2012) suggests that mantle upwellings may have dampened the

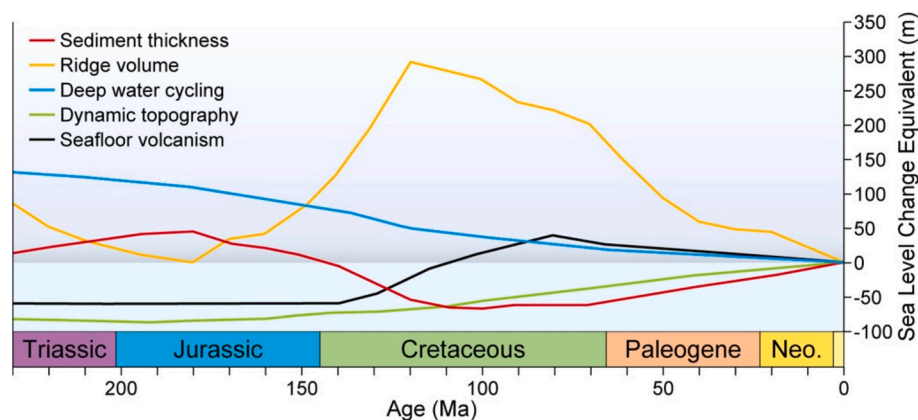


Fig. 1. Contributions to long-term SLC from different mechanisms. Main drivers of SLC for the Meso-Cenozoic (excluding ocean area and glaciation, the former being relatively invariable through the Mesozoic, and the latter became important only in the Cenozoic) as summarized by Conrad (2013) (adapted from Karlsen et al., 2019).

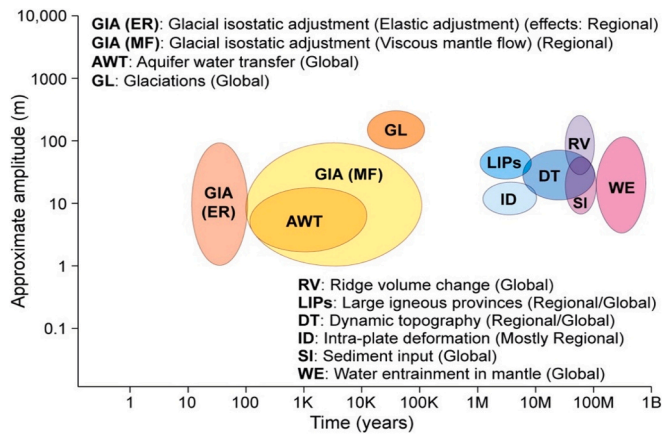


Fig. 2. Highly variable range of amplitudes and operative time-scales (on log scales) of major factors that either cause local/regional anomalies in the measure of the amplitude of SLCs (e.g., GIA, DT, ID) and those that drive long-term global SL variability (based largely on Table 1 of Cloetingh and Haq, 2015, with AWT estimates from Sames et al., 2016). [These ranges are approximations, shown for comparative purpose only and may vary considerably with time].

over all long-term SL fall by 100 to 200 m since the Late Cretaceous. However, the precise density structure of the lower mantle – whether predominantly light or dense – remains debated, introducing substantial uncertainty, as suggested by Molnar et al. (2015), who also questioned the high amplitude values ascribed to DT effects. DT, operating over multi-Myr timescales, typically generates regional amplitude anomalies with opposing effects in different areas due to long-wavelength lithospheric warping (Fig. 2).

Seawater cycling into the mantle via the hydrous minerals occurs over even longer, first-order timescales (hundreds of Myr). Over such durations, mantle cooling is thought to have enhanced water drawdown into subduction zones while reducing return flux at spreading centers. This process may have contributed to the long-term decline in global SL observed throughout the Phanerozoic (Conrad, 2013, and references therein).

Thus, it is evident that long-term SLCs, such as those spanning the

last Wilson cycle (~250 Myr), are driven by a range of processes operating across widely varying timescales. As shown in Fig. 3, estimates of SL highs and lows derived from different methodologies tend to converge primarily for the post-Triassic period. Prior to that – particularly during the Paleozoic – these estimates remain notably divergent (see, e.g., Fig. 1 in van der Meer et al., 2022). In the Triassic and Jurassic, most long-term reconstructions begin to exhibit similar trends and show increasing convergence from the Cretaceous through the Neogene, with the notable exception of discrepancies in the timing and magnitude of the mid-Cretaceous SL maximum (see Fig. 3).

In the current reappraisal, selecting the most recent continental dispersal mega-cycle as a framework for discussion is particularly appropriate. The fragmentation of Pangea began during the Mesozoic – an Era generally considered to have been largely ice-free, despite notable climatic fluctuations. These included the intensely hot and arid Triassic, the variable conditions of the early to middle Jurassic, and the predominantly warm and humid climate of the late Jurassic and Cretaceous. The limited potential for long-term water sequestration in the form of terrestrial ice during this interval allows for a clearer and more discernible signal from tectonic processes, making it especially elucidatory for our purposes. This paper does not aim to provide an exhaustive review of the subjects addressed, but rather serves as a progress report on the accelerating pace of research into past SLCs.

2. Mesozoic land- and sea-scapes

2.1. Paleogeographic and paleo-kinematic approaches

Paleogeographic and paleo-kinematic reconstructions indicate that the assembly of Pangea – a process that mosaicked continental fragments together during the Carboniferous and Permian – was essentially complete by the early Triassic. By this time, the supercontinent was topographically elevated and longitudinally aligned, with its areal extent distributed nearly symmetrically around the paleo-equator. The shape of Pangea was quasi-hemispheric: its landmass, including continental margins and epeiric seas, occupied slightly less than one longitudinal hemisphere, while the vast oceanic Panthalassa covered the remainder (see Fig. S1 in Haq, 2018). Additionally, by the early Triassic, Pangea's southern regions had shifted out of the south polar zone,

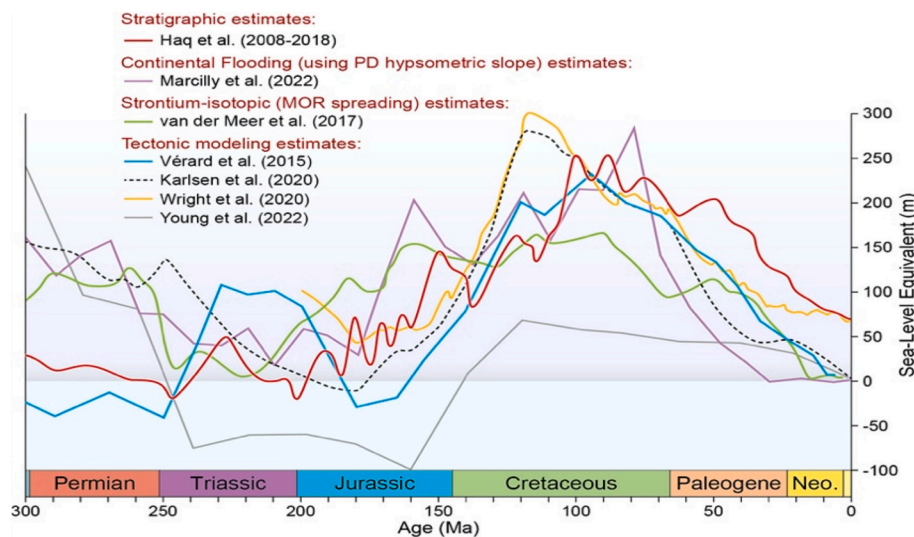


Fig. 3. Estimates of the long-term sea-level trajectories through the Meso-Cenozoic based on various methodologies (adapted from van der Meer et al., 2022, – with updated stratigraphic estimates). Stratigraphic estimates after Haq (2014, 2018, 2018a), Paleozoic updated here (after Haq and Schutter, 2008). Continental flooding estimates, using present day hypsometric slope, after Marcilly et al. (2022); Mid-ocean ridge spreading rate estimates based on Strontium isotopic data, after van der Meer et al. (2017); and various tectonic modeling estimates after Vérard et al. (2015); Karlsen et al. (2020); Wright et al. (2020); and Young et al. (2022)]. The long-term stratigraphic curve (red) assumes an ice-free world, largely reflects tectonic causes. Notice the disparity in the long-term SL curve before Jurassic. (For interpretation of the references to colour in this figure legend, the reader is referred to the web version of this article.)

accounting for the absence of glacial episodes during this period. A triangular embayment of Panthalassa on the eastern margin formed the ancestral Tethys (Neo-Tethys), which remained equatorial throughout much of the Mesozoic (Scotese and Schettino, 2017). Sparse stratigraphic evidence for climatic and SL changes (SLCs) during the Triassic comes largely from sedimentary records within the Tethyan realm (Haq, 2018a).

Early rumblings of the Pangean breakup were revealed through deep-sea drilling along the northwestern Australian margin. Rifting processes – marked by crustal stretching and block faulting – had commenced in the late Permian and continued into the early Triassic, followed by rift-related volcanism in the late Triassic (Rhaetian). This margin also exhibits a clear rift-to-drift transition during the Jurassic, with large syn-rift grabens and half-grabens infilled with shallow marine carbonates and coal measures (von Rad et al., 1989, 1992; Exon et al., 1992). Similar Late Triassic (Carnian–Rhaetian) rifting is recorded in the central Atlantic, notably in the Lusitanian Basin, where well-preserved syn-rift carbonates have been documented (Ziegler, 1989; Wilson et al., 1989), as well as in the conjugate margins of Morocco, eastern Canada, and eastern Iberia (Stapel et al., 1996). Pangea maintained its longitudinal alignment and lacked polar landmasses through the Jurassic. More conspicuous signs of breakup in the future Atlantic realm appeared in the Toarcian (late Early Jurassic, ~180 Ma), although some sources suggest an earlier onset in the Hettangian–Sinemurian (~200–195 Ma) (Frizon de Lamotte et al., 2015; Torsvik et al., 2021).

According to a recent review by Le Pichon et al. (2023), three major rotational oscillations of Pangea between the early Triassic and mid-Cretaceous (Torsvik et al., 2012; Creveling et al., 2012) significantly altered lithospheric stress fields, initiating and facilitating the supercontinent's breakup. This fragmentation was further enabled by deep lithospheric fracturing and extensive flood basalt volcanism. Pangea's considerable thickness and geographic isolation led to internal heat retention and a thermal anomaly – estimated to be as much as +150 °C relative to the asthenosphere beneath Panthalassa. As rifting and breakup progressed from the latest Early Jurassic through the mid-Cretaceous (180–100 Ma), the once-continuous subduction girdle encircling Pangea – acting as a lateral thermal barrier – was breached. This breach allowed global upper mantle temperatures to homogenize. LePichon et al. link this thermal mixing to long-term eustatic SLCs: initially low in the Triassic and early Jurassic, SLs rose as gaps in the subduction girdle developed, culminating in a peak during the

Cenomanian–Turonian. These authors propose that the mid-Cretaceous marks the transition from Pangean-style tectonics to the modern plate tectonic regime. While their model offers a novel explanation for SL variations during the assembly and breakup of Pangea, it does not elaborate on the precise mechanisms by which upper mantle thermal shifts lead to global SLCs. It is assumed that these effects occur indirectly, via changes in the ocean basins' container capacity. However, it remains unclear whether the model accounts for the exceptionally steep hypsometry of the Pangean landmass, a factor discussed in more detail below.

2.2. Hypsometric considerations

Continental hypsometry – the average elevation of land relative to global mean SL – provides valuable insight into anomalies observed in reconstructions of long-term SLCs, particularly those derived from data such as the extent of continental flooding (see Fig. 4). Hypsometry is primarily influenced by the area of emergent land and coastal gradients. As landmass area increases, such as in the case of amalgamated supercontinents, coastal slopes tend to steepen, thereby reducing the land's susceptibility to long-term marine transgressions.

When modeled through the estimated lengths and ages of ancient continental margins, past changes in hypsometry have been linked to the cycles of continental rifting and collision – so-called tectonic megacycles (Algeo and Wilkinson, 1991). It follows that by the conclusion of its assembly, Triassic Pangea would have inherited a hypsometric profile characterized by steep topographic gradients, which significantly limited the potential for marine incursions. This geomorphic condition likely contributed to the approximately 80-Myr-long SL lowstand extending from the late Permian through the early Jurassic attributed in part to reduced accommodation space along steepened continental margins, explaining the paucity of preserved marine sedimentary record for much of this interval (Haq, 2018a, b).

As an aside, and as previously discussed, Le Pichon et al. (2023) also associate this prolonged lowstand with Pangea's thermal isolation, maintained by the continuous subduction girdle encircling the supercontinent. However, their model does not explicitly incorporate the role of Pangea's elevated hypsometry. If considered, the steep hypsometric profile would reinforce their conclusion: a thermally isolated, topographically elevated Pangea would have remained resistant to flooding. Following the breaching of the subduction girdle and the subsequent cooling of the asthenosphere, as they suggest, this elevated terrain would likely have subsided, thereby increasing susceptibility to transgressive episodes as SL rose.

Recent re-evaluations of continental flooding trends – adjusted using modern-day hypsometric slopes as a correction factor – have yielded results that show improved correlation with seafloor spreading rate proxies and stratigraphic SL estimates extending back to the Mesozoic (Marcilly et al., 2022). One modeling approach – based on slope estimates of Algeo and Wilkinson (1991) – suggests hypsometry remained relatively stable over the past 300 Myr (Young et al., 2022, their abstract figure, which shows near-flat global hypsometric trends). Does this imply that hypsometric changes have had minimal influence on cumulative SL trajectories since before the breakup of Pangea?

While there is no direct record of absolute past hypsometric values, general trends can still be reasonably inferred. For instance, it is plausible that during the pre-breakup phase – due to Pangea's higher elevation and predominantly active margins and narrow shelves – hypsometric slopes would have been significantly steeper. This has important implications: current estimates of continental flooding for such periods may underestimate actual SLC, and applying steeper hypsometric corrections could lead to notably amplified SLC estimates. Developing and applying modeled reconstructions of past hypsometries could therefore improve our understanding of SL trajectories derived from continental flooding patterns, particularly during supercontinental phases when topographic gradients were likely more extreme.

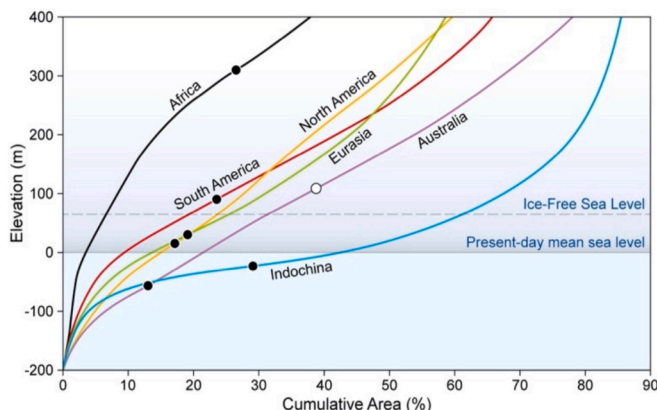


Fig. 4. Present-day (PD) coastal hypsometric curves of various continents and regions (after Algeo and Selslavinsky, 1984). Hypsometric slope (rate of change of elevation with respect to area) varies substantially between continents (dots indicate inflection points). This implies large-scale elevation of Africa and subsidence of Australia compared to other continents. Due to lack of data on past hypsometric slopes, models end up using present-day slope analog for the long-term SLC estimates even for the amalgamated Pangea, which can produce anomalous results.

2.3. Seafloor production rates

The Cretaceous Period was marked by the emergence of narrow seas between the rifted fragments of Pangea, resulting in a substantial expansion of the mid-ocean ridge system and the proliferation of shallow marginal and epeiric seas. Reconstructions of seafloor kinematics – such as mid-ocean ridge volumes – are typically derived from full-plate models. However, these reconstructions are subject to significant uncertainties, particularly for deep-time intervals, due to the limited direct evidence of ridge extent. Beyond the most recent dispersal cycle, even reconstructions of subduction zones become problematic, as the relevant oceanic lithosphere has been largely subducted and assimilated into the mantle. As a result, much of the modeling for earlier periods remains informed conjecture.

Despite these caveats, tomographic and geodynamic data suggest that crustal production rates in the past – driven predominantly by ridge accretion, subduction, and large igneous province (LIP) emplacement – were significantly higher than present-day rates. For instance, [van der Meer et al. \(2017\)](#) estimated that the total length of subduction zones during the Early Cretaceous was approximately double that of today. In contrast, [Müller and Dutkiewicz \(2018\)](#) contend that subduction zone lengths have varied by only about 20 % since the Triassic. These starkly different conclusions stem from divergent methodologies, yet such inconsistencies hamper efforts to constrain geodynamic models with confidence.

Plate motion reconstructions by [Müller et al. \(2016\)](#), which extend back to the early stages of Pangea's breakup, indicate relatively slow average absolute plate velocities (< 5 cm/yr) during the Triassic and Jurassic. These rates nearly doubled (to 9–10 cm/yr) in the Early Cretaceous (Berriasian–Barremian) due to multiple LIP emplacements and potentially also due to enhanced plate-mantle coupling. Further accelerations are observed around the Albian–Cenomanian boundary – particularly in the Indian Ocean region, possibly related to subduction initiation along the southern Eurasian margin – and again in the Campanian, when Greater India began its rapid northward drift. This trend of increasing motion was abruptly reversed upon India's collision with Asia in the Ypresian ([Haq, 1988](#)).

Rifting and the formation of new ocean basins inherently alter the ocean's container volume, thereby impacting long-term SLCs. Estimates of the resulting SL rise due to container size reduction vary widely, ranging from ~ 78 m since the beginning of the Cretaceous ([Müller et al., 2008](#)) to as little as ~ 21 m since the initial breakup of Pangea ([Kirschner et al., 2010](#)). This ambiguity arises from several complicating factors. For one, newly formed ocean basins initially displace older ones; during early stages of basin development, the increased volume can accommodate water, thus contributing to some SL lowering at first. But after sustained accretion at spreading centers leads to significant ridge volume do the basins effectively reduce global container capacity and affect a reversal in the SL trajectory. Moreover, acceleration in subduction rates – driven by enhanced ridge push – must also be factored into these dynamics (see also, [Young et al., 2022](#)).

Additional complexities include asymmetries at spreading centers, variable sedimentation rates, and the role of back-arc basins, which constitute an essential component of the subduction system. When these factors are integrated into reconstructions, more comprehensive estimates suggest that the cumulative SLC driven by ocean basin volume variation since the onset of Pangea's breakup approaches ~ 200 m ([Wright et al., 2020](#)).

2.4. Mantle-lithosphere dynamics and its impact on surface topography

Dynamic topography (DT) – broad-wavelength, long-timescale expression of mantle convection acting upon the overlying lithosphere – has been estimated to reach amplitudes of up to ~ 2 km, with wavelengths extending as far as 5000 km ([Flament et al., 2013](#)). Yet at these large scales, the true bulges rarely exceed about 900 m in relief ([Davies](#)

[et al., 2019](#); [Flament, 2019](#)). The elevated Triassic terrain of Pangea, for instance, may be attributed in part to dynamic topographic uplift, potentially driven by thermal insulation effects beneath the supercontinent ([Young et al., 2022](#); [Le Pichon et al., 2023](#)).

It is important to distinguish DT from more stable isostatic topography, which is controlled by density differences within the lithosphere. In contrast, DT arises from mantle flow – specifically upwelling and downwelling – that determines the location and magnitude of dynamically elevated or depressed surface regions. DT is often expressed as a regional anomaly in stratigraphic reconstructions of SLC. However, if DT significantly alters oceanic bathymetry, it can also influence the global ocean basin volume – thus introducing a secondary control on long-term SLC estimates. For example, by combining the evolving age distribution of the ocean crust since the Late Cretaceous with DT (and geoidal corrections), [Spasojević and Gurnis \(2012\)](#) concluded that DT partially offsets the predicted ~ 250 – 300 m SL fall from seafloor cooling, yielding a maximum eustatic deviation of about 286 m at ~ 80 Ma (with DT and geoid contributing together). Nonetheless, [Conrad \(2013\)](#) has argued that such estimates may be overstated, suggesting that the contribution of DT to global SLC may be negligible when considering seismological data indicating that lower mantle structures may be denser than previously assumed ([Deschamps and Trampert, 2003](#)). Lingering uncertainties persist regarding how DT reacts to assumed variations in crustal architecture ([Boschi et al., 2010](#)). [Davies et al. \(2019\)](#) underscore that it is the lithosphere's internal structure that chiefly governs the resulting residual topography of the crust. [Stephenson et al. \(2024\)](#) actually show that beyond crustal thickness and density contrasts, a substantial component of continental residual topography is supported by the buoyancy structure of the lithosphere and the underlying convecting mantle. In particular, they demonstrate that variations in lithospheric thickness – together with sub-plate mantle convection – constitute the dominant control on those residual elevation anomalies.

Following the fragmentation of Pangea in the Early Jurassic, the individual continental blocks – now separated and subject to their own dynamic regimes – began to develop distinct average elevations and hypsometric gradients. Some of these landmasses, such as Australia and Africa, deviated significantly from global hypsometric trends ([Gurnis et al., 1998](#); [Moucha and Forte, 2011](#)), complicating the derivation of a consistent, global-scale long-term SL curve based solely on flooding or present-day hypsometric data (see [Fig. 5](#)). To address this complexity, [Marcilly et al. \(2022\)](#) applied modern hypsometric slopes to refine continental flooding-based reconstructions (e.g., [Kocsis and Scotese, 2021](#)). While this correction improved correlations with stratigraphic SLC estimates for the Paleozoic through Cenozoic, it still diverged from tectonically derived SL models – particularly for deep-time intervals, where direct seafloor evidence is generally lacking. Importantly, [Marcilly et al.](#) also acknowledged that adjusting flooding reconstructions to account for steeper hypsometric gradients in the past – such as during the Pangean phase – would yield significantly higher inferred SL fluctuations. Their modern hypsometry-based flooding curve generally aligns with stratigraphically reconstructed long-term SL trends, but diverges from those extrapolated from geodynamic and tectonic models in earlier geological periods.

2.5. The role of plumes

Recent advances in seismic tomography have provided new insights into the geometry and nature of mantle plume emplacement. Notably, large-scale plumes, such as the Iceland Plume, have been observed rising from the core-mantle boundary beneath the North Atlantic. This plume, with side lobes extending beneath the Norwegian rifted margin and the northwestern part of the British Isles, exemplifies the scale and reach of plume activity ([Rickers et al., 2013](#)). Additionally, high-resolution seismic data have revealed the widespread occurrence of secondary mantle plumes originating from the mantle transition zone – the boundary between the upper and lower mantle ([Kuritani et al., 2019](#);

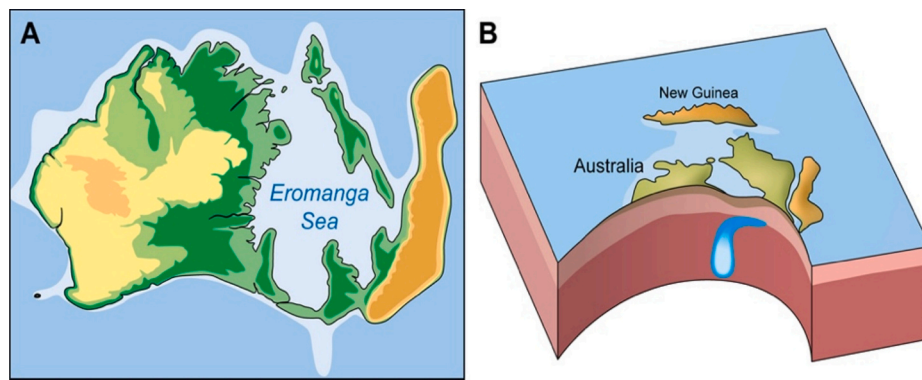


Fig. 5. Conceptual example of the effects of dynamic topography: A: The mid-Cretaceous Eromanga Seaway created by dynamically modified topography of Australia – DT caused epicontinental seaway (between ~125 and 95 Ma) had an average depth of between 50 and 100 m. Paleogeographic reconstruction of the seaway (at ~100 Ma) with northward opening and altered drainage (modified from Harrington et al., 2019). B: A cut-out of the conceptual model of the cold subducting plate downwelling in the mantle while traversing underneath Australia, pulling down the lithosphere to produce the eastern interior seaway (up to 300 m in depth) in the mid Cretaceous (modified from Gurnis, 2001).

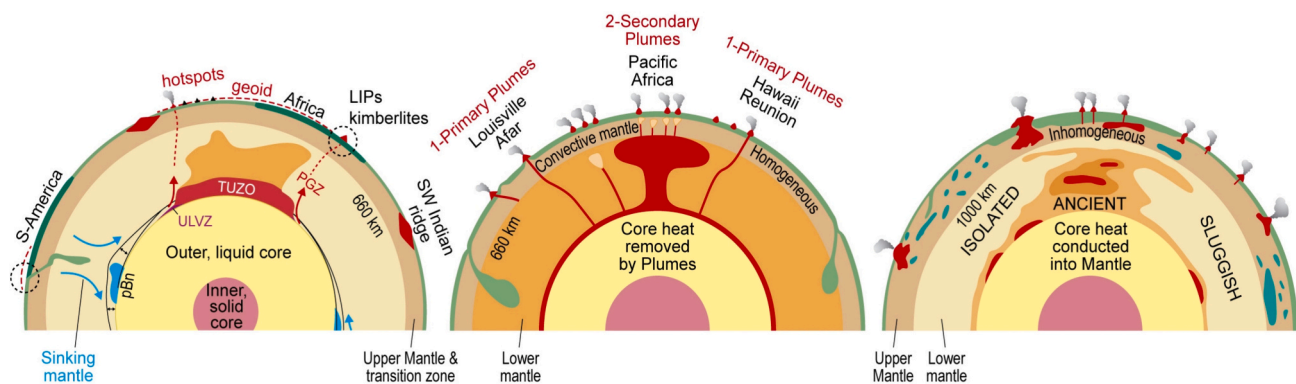


Fig. 6. Three conceptual models of Earth's interior illustrate that plumes are multiscale and can originate at different levels of the mantle. Depending on their size they may or may not influence changes in the oceanic container capacity. Secondary plumes sourced from the water-rich mantle transition zone have large water carrying capacity which also enhances their lithosphere penetration capability (adapted from Koptev et al., 2021).

Koptev et al., 2021; Fig. 6). This transition zone, with its high fluid content (Koppers et al., 2021), acts as a conduit for the ascent of secondary plumes through the lithosphere, particularly in rifted margin environments where plume emplacement can result in significant vertical motion at the ocean-continent boundary (Francois et al., 2018; Cloetingh et al., 2022), with substantial implications for local hypsometry (as discussed above).

An inventory of primary and secondary plumes, compiled from seismic tomography studies (Montelli et al., 2006), reveals that the majority of primary plumes are deep-seated beneath the oceans, whereas secondary plumes tend to be associated with intracontinental or rifted margin settings. Furthermore, a recent study that examined the distribution of basalts in ophiolites over the past 2 billion years confirms that plumes were consistently active beneath oceanic regions during the Pangean era (Doucet et al., 2019). This suggests that plume-related topographic alterations could have had a more significant role in influencing the oceanic basin's container capacity than previously assumed.

2.6. Large igneous province emplacements

Large igneous provinces (LIPs), particularly those driven by plumes, can significantly alter the volumetric capacity of the oceanic container, especially if the outpourings are of substantial size (Koptev and Cloetingh, 2024). During the Mesozoic, numerous igneous eruptions formed both continental and oceanic LIPs (Ernst et al., 2021). While many of these outpourings were relatively modest in scale, the larger oceanic

LIPs directly impacted SLC. With few exceptions (see below), the extent of oceanic LIPs was typically limited. Continental LIPs, although more prominent in size, are indirectly relevant to SLC as they affect regional hypsometries, influencing local SL measurements.

The most notable oceanic LIPs that substantially impacted the oceanic container's volume ($>1.0 \text{ M km}^2$, approximately half the size of the Deccan Traps) include: 1) Bunbury-Comei and Kerguelen-Rajmahal LIPs (Valanginian, with successive Albian and Coniacian pulses): These mixed oceanic-continental outpourings together covered approximately 1.6 M km^2 . 2) Arctic Ocean LIP (end of Barremian, with an additional pulse at the end of Cenomanian): This vast, mixed oceanic-continental outpouring spanned about 7.4 M km^2 , affecting the high Arctic and parts of North America, Europe, and Asia. 3) Ontong-Java and Nui Plateaus (mid-Aptian): A major oceanic outpouring that exceeded 6.4 M km^2 in area, which also contributed to oceanic anoxia. [If Ontong-Java is combined with Manihiki and Hikurangi Plateaus – as they were a single feature before separating (Taylor, 2006) – the size would be, of course, much larger]. 4) Caribbean-Columbian Oceanic LIP (partially straddling the Turonian and Coniacian Stages): Covering 1.54 M km^2 , this large oceanic outpouring had notable impacts on the oceanic volume. Other oceanic igneous outpourings were smaller and of lesser consequence for SLC discussions. The Cretaceous-Paleogene (K–P) boundary Deccan Traps were largely a continental outpouring, with a small oceanic component.

During the end-Permian through Mesozoic interval, major igneous outpourings were predominantly continental, such as: Siberian Traps (end-Permian): Extending over 3.47 M km^2 ; Central Atlantic Magmatic

Province (end-Triassic): A vast outpouring spanning 11.28 M km^2 across North America, Europe, Africa, and South America; Karoo LIP (late Early Jurassic): Encompassing 3.15 M km^2 across South Africa and Antarctica; Parana-Etendeka LIPs (early Cretaceous): Stretching 3.47 M km^2 across South America and Africa; Deccan Traps (K–P boundary): A largely continental outpouring covering 1.85 M km^2 in India, with smaller oceanic contributions. Although many major continental LIPs, like the Siberian and Deccan Traps, did not directly precede continental breakup (Koptev and Cloetingh, 2024), their influence on regional hypsometric slopes was most likely significant. These regional alterations could have influenced the local floodability of the continents, and, by extension, affected global SLC measurements.

3. Deep-water recycling through the mantle

The long-term cycling of water via hydrous minerals in the mantle occurs over vast time scales, often spanning billions of years. As the mantle cools over long periods, the drawdown of water into subduction zones increases, while replenishment at the spreading centers and other seafloor outpourings decreases. This process may, in part, explain the long-term decline in SL throughout the Phanerozoic. Water and sediments from the subducting hydrated slabs eventually return to the ocean and atmosphere through volcanic activity. It is safe to assume that during the stable (assembled) phase of a supercontinent, deep-water fluxes generally do not change significantly.

Water transfer from the ocean to the mantle intensifies only after the breakup begins and new ridges are accreted, which in turn push and accelerate regassing into subduction zones. Eventually, presumably after some time lag, degassing will return the water to the ocean (Karlsen et al., 2020).

The role of mantle water cycling in SL changes is credible, particularly on relatively long timescales (tens of Myr). The quantity of water carried into subduction zones depends on slab characteristics such as composition, volume, age, subduction velocity, and the nature of hydrous minerals present (Karlsen et al., 2020), with subduction velocity playing a major role (Magni et al., 2014). But, our regassing-degassing inventories are patchy at best. For example, one bold estimate suggests that deep-water cycling into the mantle since 250 Ma could account for as much as 240 m of SL drop (Young et al., 2022). Earlier, Parai and Mukhopadhyay (2012) had used noble-gas signatures and water-flux constraints to argue that the modern deep-mantle water cycle is net regassing, with more water – almost twice the amount – being driven downward at trenches than that being returned to the surface by degassing on the seafloor. Nevertheless, such guesswork of tracking down estimates and time scales of deep-water fluxes are fraught with uncertainties, and these could alter such approximations by up to 50 % (Peslier et al., 2017).

Understanding the flux of water returning to the ocean requires detailed knowledge of oceanic crust production rates, which depend on the extent (length and volume) and spreading rates of the ridges, as well as contributions from hotspot and LIP volcanism. Modeling these factors in deep time is challenging, as direct evidence or indirect indicators (such as tomographic imaging) are often unavailable, leaving estimates based on theoretical assumptions.

It has been suggested that long-term SLCs over hundreds of Myr, corresponding with supercontinental assembly and breakup cycles, are influenced not only by changes in ocean basin volume but also by variations in the rates of water flux into and out of the mantle. These fluxes are governed by changes in the extent of subduction zones and mid-ocean ridge systems (Worsley et al., 1984; Karlsen et al., 2019). However, there are significant uncertainties in these models, particularly regarding the amount of water currently present in the mantle compared to surface water. Estimates range from the mantle containing an amount equivalent to one ocean mass to as much as ten times that amount (Nestola and Smyth, 2016; Karato et al., 2020).

Recent high-pressure experiments have suggested that deep-water

cycling, through the transport of metasomatic chlorite-rich rocks at subduction zones, may have led to a secular non-equilibrium in the mantle, potentially increasing its water content over time (Hermann and Lakey, 2021). Additionally, recent in-situ findings at the Mariana Trench indicate that water input into the mantle may be three times higher than previously estimated (cf. van Keken et al., 2011 vs. Cai et al., 2018). Despite these discrepancies, it is widely agreed that there is a net flux of water into the mantle. Current disparity in flux rates also implies such imbalance in the past, changing with global tectonic rearrangements (e.g., Korenaga et al., 2017; Peslier et al., 2017; Karlsen et al., 2019).

Recent models of water flux into and out of the mantle, based on downwelling water flux from slab age and subduction velocity, suggest a wide range for current mantle water content (Karlsen et al., 2019). These models, derived from current tectonic plate reconstructions (Matthews et al., 2016; Müller et al., 2016), predict a long-term drop in SL, primarily attributed to ocean-mantle water imbalances, with estimates placing this drop at approximately 130 m. However, it is unclear if these models account for isostatic compensation of the seafloor due to water transfer between reservoirs. The majority of regassing into the mantle occurred before 70 Ma, during the major phase of Pangean breakup, when subduction rates and the influx of water into the mantle were accelerated. The formation of new ridge systems would have enhanced this process, creating larger ocean basins that increased container capacity and contributed to the overall SL drop (Karlsen et al., 2019). However, these new ridges also provided greater opportunities for hydrous flux from the mantle to the ocean, which could counterbalance the SL drop. These opposing factors are not always clear in current models. Our understanding of the dynamics of ocean ridges and trenches, and how they control deep-water fluxes, remains in its early stages. Further research into these processes should be a key focus in future modeling efforts.

4. Glacio-eustasy

For a long time, glaciation – specifically the sequestration of water as ice on land – has been considered the primary driver of third-order and higher-frequency eustatic cycles. There is substantial evidence supporting glacio-eustasy since at least the mid-Eocene, with the long-period modulation of Milankovitch harmonics widely recognized as the root cause. In this framework, the polar positioning of land, in addition to climate and CO_2 levels, plays a crucial role in enabling the Earth to enter a glacial mode. Paleogeographic reconstructions of the Mesozoic show that the Pangean landmass was mostly far from the poles (Scotese, 2021). Combined with high CO_2 levels (van der Meer et al., 2017) and generally warm climates, this severely reduced the potential for major glaciation during this period.

However, recent model reconstructions based on paleo-latitudes of polar ice fronts and correlations with land and shelf margins (van der Meer et al., 2022) suggest that at least some quasi-perennial ice accumulation may have occurred in the Late Jurassic and Cretaceous (Fig. 7A). Additionally, a modeling study by V  rard (2024) using a linear fit of stratigraphically-derived SLC data, de-trended long-term variations, and a 60.6-m baseline to separate hothouse from ice-house conditions, proposes that secular ice-house conditions may have existed throughout the Phanerozoic (Fig. 7B).

Such model conclusions notwithstanding, there is significant, albeit indirect, evidence supporting the idea of an essentially ice-free Mesozoic and early Paleogene. For example, $\delta^{18}\text{O}$ isotopic data strongly suggest hothouse climates from the mid-Aptian onward, with extremely warm bottom temperatures ($>20^\circ\text{C}$) at mid-bathyal depths, and surface waters at 60°S paleo-latitudes reaching $30\text{--}32^\circ\text{C}$ during peak SL highs in the Cenomanian-Turonian. Cooler conditions returned in the Maastri  chtian, making glaciation in the Late Cretaceous a very unlikely scenario (Haq and Huber, 2016). Nonetheless, it has been suggested (Cloetingh and Haq, 2015; Haq and Huber, 2016) that glaciation in the Late Cretaceous cannot be completely ruled out, particularly under one

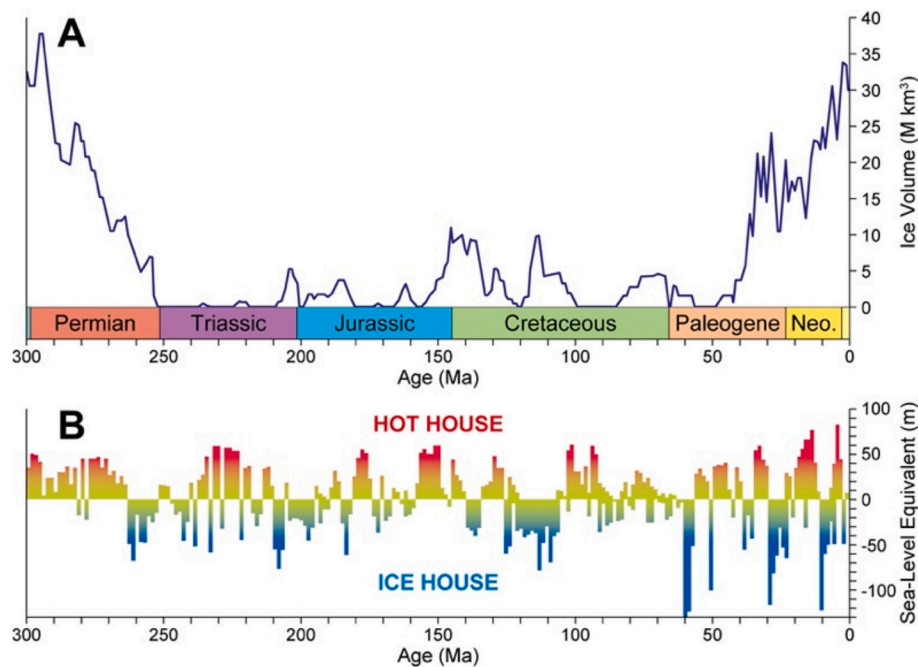


Fig. 7. Glacial episodes in the Mesozoic hinted by modeling studies. A: Ice volume estimates based on paleo-latitudes of polar ice front and correlation with land and shelf margins (modified after [van der Meer et al., 2022](#)). Compare the Permian and late Paleogene to Recent peak ice volume estimates with those in the Mesozoic, which amount to about 1/3 to 1/6 values of the Peak Permian and Neogene. B: Inferred icehouse (glacial) and hothouse (ice free) regimes based on 60.6 m base line of the de-trended eustatic curve with polynomials removed (modified after [Vérard, 2024](#)).

scenario: the presence of Antarctic highlands with sufficient altitude to sequester substantial amounts of water as ice, potentially affecting eustatic change. Testing this hypothesis would require tomographic imaging of West Antarctica, followed by forward modeling, to determine whether a high plateau could have existed on the continent during the Late Cretaceous.

While such hypothetical exercises suggesting quasi-perennial or ephemeral ice accumulations remain controversial, they reignite the discussion about the potential presence of glaciation in the so-called “ice-free” Mesozoic world. In the Paleogene, recent inferences from the oxygen-isotopic record argue for an earlier onset of Antarctic ice accumulation (middle Eocene rather than late Eocene) ([Dawber and Tripathi, 2011](#); [Haq and Ogg, 2024a, 2024b](#)) and possibly even minor ice-house phases in the early Eocene ([Miller et al., 2024](#)).

At this stage, however, the assumption that there was little or no land-based ice during the Triassic, most of the Jurassic, and the Paleocene – except perhaps for the latest Jurassic and Early Cretaceous, which remains uncertain – is a factually reasonable position, pending more convincing evidence to the contrary.

5. Long and short-term variations of sea level

It should be noted that while the discussion above has largely focused on the long-term (2nd-order) SLCs, in this section we not only discuss the long-term trends but also include shorter-term (3rd- and 4th-order) variations. Fourth-order and higher frequency cycles have been documented throughout the Phanerozoic, discernable when sedimentation rates are high enough for such detailed resolution of the stratigraphic record ([Haq and Ogg, 2024b](#)).

Cyclic order in sedimentary sequences can be summarized as follows: 1st-order sequences are driven by plate assembly-dispersal megacycles (duration 250–300 Myr), while 2nd-order sequence are affected by seafloor tectonics related to lithosphere-mantle interactions (several 10s of Myr); 3rd-order cycles are caused largely by the long-period modulations of the Milankovitch periodicities (0.5 to 2.5 Myr); and 4th- and 5th-order cycles (~410 and 100 Kyr, respectively) seem to line up with

multiples of precession, obliquity and eccentricity cycles of the Earth’s orbit. The sedimentary record shows the combined harmonics of all of these periodicities. In this section we present updates of the stratigraphically determined Mesozoic eustatic curves that have been recalibrated to the latest version of the numerical time scale (GTS2020).

5.1. Mesozoic sea-level variations (updated)

One notable feature of the long-term SL trajectory from the late Permian through the Triassic and into the early Jurassic, a span of nearly 80 Myr (while Pangea remained largely assembled), is the sustained lowstand that marked the longest duration of low SLs in the Phanerozoic ([Haq, 2018a](#)). As previously discussed, the steep hypsometric slopes and reduced continental margin extent during the supercontinental phase of Pangea likely contributed to the low floodability of the landmass, as well as the limited preservation of marine sediments during this period.

Throughout much of the Triassic, when Pangea was in a fused state, SLs remained at their lowest, staying close to or below present-day mean sea level (PDMSL), rising only about 50 m above this level in the late Carnian to early Norian interval ([Fig. 8](#)). Another prominent feature of Triassic eustasy is the scarcity of third-order cycles, which are notably long in duration – averaging around 5 Myr for the Middle and Late Triassic – compared to the ~1.29 Myr per cycle seen in the Mesozoic as a whole. This paucity of marine sediments can be attributed to the elevated position of Pangea, and as mentioned earlier, resulting from thermal isolation and heat anomalies in the asthenosphere beneath the thick supercontinent ([Le Pichon et al., 2023](#)). Most of the stratigraphic documentation for the Pangean lowstand eustatic cycles comes from the carbonate sections along the tropical Neo-Tethyan margins ([Haq, 2018](#)). Despite the low number of Middle and Late Triassic third-order sequences, their boundaries are typically marked by major SL falls (more than 75 m, many exceeding 100 m below PDMSL).

The long-term SL trajectory mirrors the breakup patterns of Pangea. The persistent lowstand trend of the Triassic extends into the early Jurassic, dipping to PDMSL at the Pliensbachian-Toarcian boundary. This trajectory shifts as Pangea begins fragmenting in the Early Jurassic.

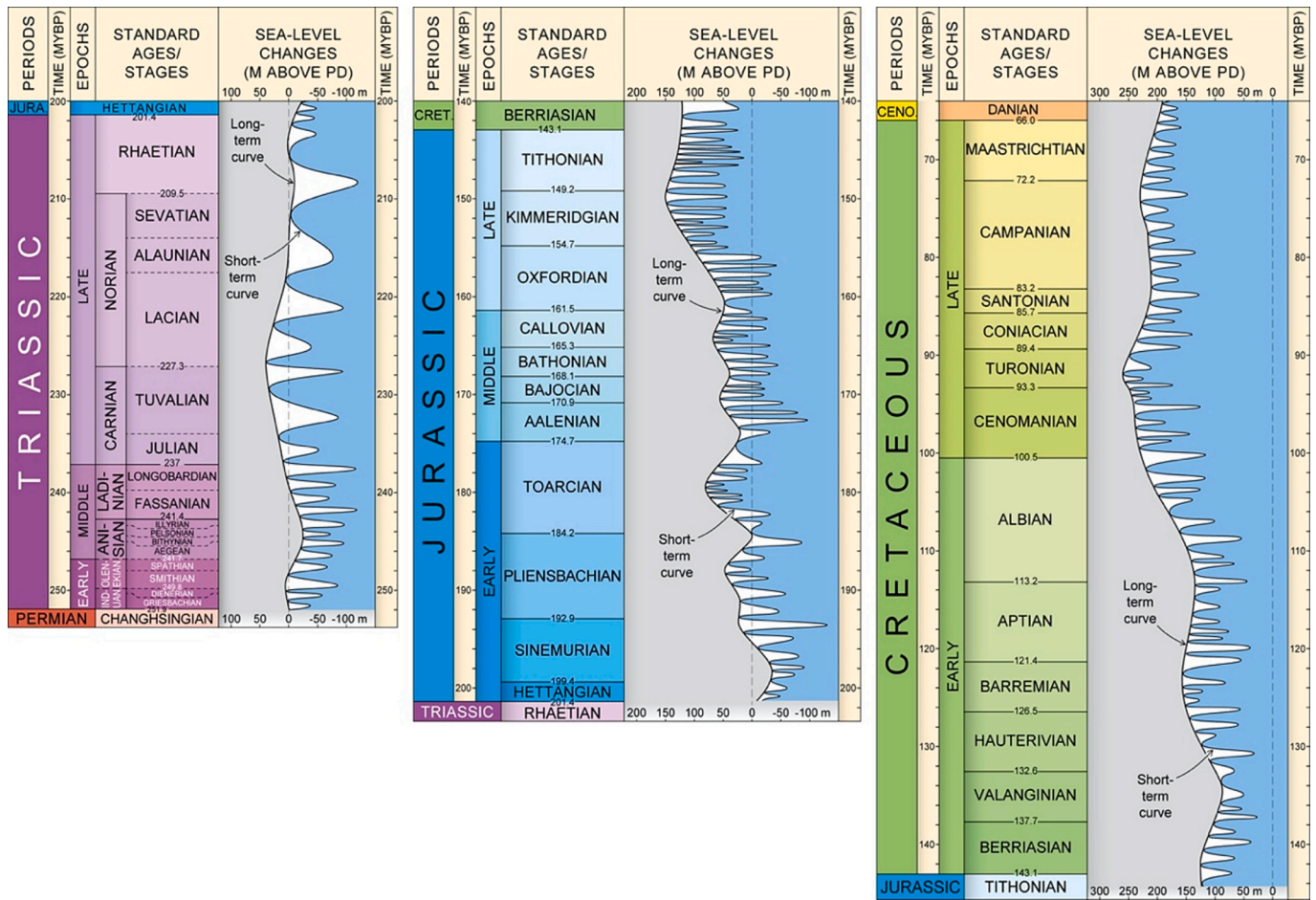


Fig. 8. Reappraised long-term (2nd-order) and short-term (mostly 3rd-order) SL variations through the Mesozoic (Triassic reappraisal, after Haq, 2018; Jurassic, after Haq, 2018a; and Cretaceous, after Haq, 2014).

The mid-Toarcian sees a peak in SL, coinciding with major rifting in the central Atlantic region of Pangea. This is followed by two smaller peaks in the Middle Jurassic, and thereafter, a sharp rise in SL during the Late Jurassic, beginning in the mid-Oxfordian and extending into the Kimmeridgian. SLs reached another peak (~150 m above PDMSL) near the Kimmeridgian-Tithonian boundary. Many Jurassic stratigraphic sections display fourth-order cyclicity (~410 Kyr multiples of orbital eccentricity), highlighting the significant role of climate in shorter-term eustatic variations (Haq, 2018a).

During the Cretaceous, when crustal production rates on the seafloor were at their highest (see Fig. 1), long-term SLs were also at their highest (Fig. 8), with a sustained high for over 65 Myr (from Hauterivian to Maastrichtian). Two prominent troughs in this overall trend of sustained high SLs occurred in the Valanginian and near the Aptian-Albian boundary. SLs reached their zenith in the late Cenomanian-Turonian, potentially representing the highest eustatic levels in the entire Phanerozoic (Haq, 2014). The Cretaceous period was characterized by numerous third-order and higher-frequency depositional cycles, with an average duration of ~1.18 Myr. These cycles include several intervals where fourth-order cyclicity predominates, underscoring the strong climatic influence on Cretaceous eustasy. Many Cretaceous events, particularly those associated with fourth-order variations, also show minor (<25 m) amplitude rises and falls, which have been attributed to limno-eustasy (the transfer of water between aquifers on land and the ocean) (Wagreich et al., 2014; Wendler and Wendler, 2016). Given the generally warm and wet climate of the Cretaceous, this factor warrants serious consideration and may prove to be an important contributor to SLCs under the greenhouse climate conditions of the time.

5.2. Third-order and higher-frequency cycles

Our ability to resolve stratal and structural details in seismic-stratigraphic profiles, particularly for interpreting third-order and higher-frequency depositional cycles, has steadily improved over the past few decades. This progress was recently highlighted by Xu and Haq (2022), who introduced new concepts and interpretive procedures that promise to enhance seismic facies and lithofacies analyses. These innovations are especially valuable for identifying small-scale structural features and rock types that were previously not apparent in seismic images of sedimentary edifices. The new techniques allow for more precise restoration of original depositional architecture and improved seismic slice image analysis.

In parallel, time-series analyses of stratigraphic data from various sources have revealed recurring patterns suggesting that long-period modulations of orbital obliquity and eccentricity cycles (i.e., 1.2 and 2.4 Myr, respectively) are common in many datasets. This includes Cenozoic oxygen- and carbon-isotopic records (Lourens and Hilgen, 1997; Wade and Pälike, 2004; Pälike et al., 2006; Liebrand et al., 2016; Kocken et al., 2019), the sequence stratigraphic record (Boulila et al., 2011; Liu et al., 2019; Rampino and Caldeira, 2020; Haq and Ogg, 2024a), the fossil record (van Dam et al., 2006), and deep-sea hiatuses (Dutkiewicz et al., 2024).

These developments have provided a clearer understanding of the causal relationship between astronomical factors and stratigraphy. A strong indication has emerged that much of the third-order cyclicity, especially within the 1.2 to 2.4 Myr range, may be largely driven by the Milankovitch grand periodicities, which are controlled by climate

variations caused by changes in the Earth's orbital parameters around the Sun. Spectral analyses have further confirmed earlier observations that, during non-glacial (greenhouse-hothouse) intervals, the orbital eccentricity signal (and its multiples) dominates, while during glacial (icehouse) intervals, the obliquity signal is more prevalent (Boulila et al., 2011).

6. Discussion and outlook

Understanding SL trajectories is central to comprehending Earth System Dynamics. Deconvolving past SLCs is crucial for unraveling the multi-scale nature of ancient Earth System processes and their spatial and temporal interactions. We have only just begun to appreciate the complexities of these interactions, which involve both deep Earth processes and surface processes, as well as the transfers of materials between reservoirs. Ambiguity often arises when the multi-scale nature of these processes and their final expression in the stratigraphic record is overlooked.

Reconstructing SLC trajectories in deep time presents considerable challenges. In such cases, where seafloor features from ancient times are largely inaccessible – either having been recycled into the mantle or obscured – reliance on proxies and model reconstructions is highly assumption dependent. This creates uncertainty in our interpretations. For example, very few old Mesozoic seafloor features remain accessible, having been largely subducted, with the notable exception of rare obducted ophiolites. In plate reconstructions, the location and extent of mid-ocean features, particularly spreading centers, can vary significantly. While post-rift spreading between drifting continental fragments can be inferred, the placement of ridges outside these bounds remains speculative. Thus, estimating oceanic production rates with precision may not be feasible, and these rates cannot be used reliably for reconstructing SLC trajectories based on a singular methodology. This may explain the divergent long-term SL estimates in deep time, based on different models (see Fig. 1, pre-Jurassic portion).

The Triassic through early Jurassic period is characterized by rifting processes that initiated the fragmentation of Pangea. During this time, the steep hypsometries of the Triassic began to diminish, creating new accommodation space for sediments while increasing the floodability of continental margins. This combination of factors contributed to a long-term SL rise from the mid-Jurassic onwards, which continued into the Cretaceous. In the Mesozoic, long-term SL curves tend to converge, although differences in amplitude estimates remain.

Recent developments include time-series analyses of SL curves in conjunction with tectonic, sedimentological, and fossil biodiversity data. Several potential connections have been identified. For example, spectral analysis has revealed a 32-Myr periodicity in sequence-stratigraphic boundaries (SL fall events) recorded in Phanerozoic sections from the Canadian Arctic (Rampino and Caldeira, 2020), suggesting a connection between tectonics and Milankovitch cycles. Other studies have uncovered a 35–36 Myr cyclicity in SLC and subduction rates, which appears to correlate with long-period Milankovitch harmonics, hinting at a coupling between Earth's interior dynamics and surface processes mediated by orbitally-paced climate cycles (Boulila et al., 2021) (Fig. 9).

Additionally, the periodicity shared between SLC, tectonics (e.g., ridge extent, crustal production, subduction rates), macro-stratigraphy (e.g., total carbonate areas), and marine biodiversity patterns over the past 250 Myr has led to the hypothesis that a common forcing mechanism – such as convection-driven changes in slab velocities – could be responsible for this cyclicity. These changes may influence deep-water cycling, offering a potential link between Earth's interior processes and surface dynamics (Boulila et al., 2023).

Statistical manipulations of different datasets, derived from widely varying approaches, present significant challenges due to the inherent uncertainties within each methodology. These uncertainties include undetected gaps in both temporal and spatial data, differing concepts

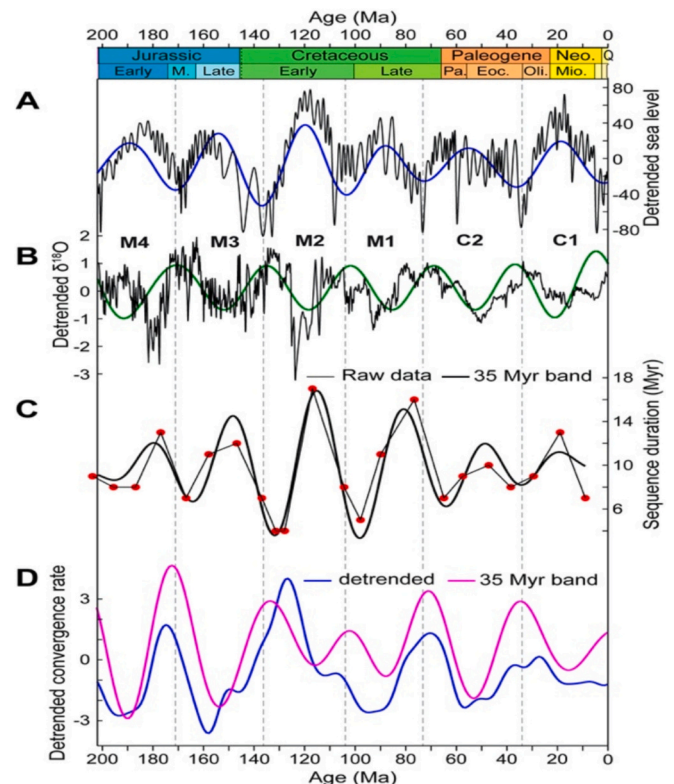


Fig. 9. Time series analysis of different geological datasets attributed to different authors that shows common 35 Myr cyclicity (adapted from Boulila et al., 2021) (each dataset is shown along with a 35 Myr bandpass filter). A. Detrended eustatic sea level data; B. Detrended oxygen-isotopic data; C. Duration of major sequence boundaries in Canadian Arctic basins; D. Detrended convergence rate (subduction) dataset. (For individual references to datasets, see Boulila et al., 2021).

and assumptions among data gatherers, varying rigor in data collection, and a lack of internal consistency across datasets from multiple workers. Additional factors such as potential taxonomic and sampling biases in fossil data further complicate the matter. As a result, these datasets cannot always be taken at face value. However, efforts to seek commonalities in trends and hypothesize potential connections, despite their conjectural nature, can foster vibrant debate and stimulate further inquiry. Such engagement is invaluable for the progress of science.

Another significant limitation lies in data variability, both in terms of quality and geographic coverage. Greater emphasis is needed on acquiring new data from regions with limited information, such as Africa, South America, and Antarctica. Industry holds valuable legacy data that could greatly benefit scientific research. Academia and national science agencies must actively engage with the industrial sector, urging it to unlock critical data that can propel scientific discovery and serve the broader good. Information gathered through public funding should not languish in closed coffers – it must be swiftly and widely disseminated, especially to support the global research community. Every scientific publication that contains reusable, high-value data and insights should be freely accessible to all. When such knowledge is kept behind barriers, it becomes the privilege of a few, stalling the collective progress of science.

In an era of mounting climate uncertainty, sea-level change research stands as one of the most urgent geoscientific endeavor. The record of past sea-level shifts offers an indispensable lens through which we can anticipate future environmental upheavals. Now more than ever, we must commit serious intellectual effort and robust funding to this essential field. The cost of inaction is far too high.

Declaration of competing interest

The authors declare that they have no known competing financial interests or personal relationships that could have appeared to influence the work reported in this paper.

Acknowledgements

We would like to acknowledge the use of research facilities at Sorbonne University, Utrecht University, the Smithsonian Institution in Washington, DC, and the Institute of Earth Physics and Space Sciences in Sopron during our numerous deliberations over the years. We are grateful to Nicolas Flament and James Ogg for their reviews that helped improve the quality of the paper. We are also grateful for the insightful discussions with Fred Beekman, Alex Koptev, Pietro Sternai, and Slah Boulila. Additionally, we appreciate the diligent work of Alexandre Lethiers at Sorbonne in drafting the figures included in this study.

Data availability

No data was used for the research described in the article.

References

- Algeo, T.J., Sclafavinsky, K.B., 1984. Reconstructing epeirogenic and eustatic trends from paleo-continental flooding data. In: Haq, B.U. (Ed.), *Sequence Stratigraphy and Depositional Response to Eustatic, Tectonic and Climatic Forcing*. Kluwer, pp. 209–246.
- Algeo, T.J., Wilkinson, B.H., 1991. Modern and ancient continental hypsometries. *J. Geol. Soc. Lond.* 148 (4), 643–653.
- Boschi, L., Faccenna, C., Becker, T., 2010. Mantle structure and dynamic topography in the Mediterranean Basin. *Geophys. Res. Lett.* 37 (20).
- Boulila, S., Galbrun, B., Müller, R.D., Pekar, S.F., Browning, J.V., Laskar, J., Wright, J.D., 2011. On the origin of Cenozoic and Mesozoic “third-order” eustatic sequences. *Earth Sci. Rev.* 109 (3–4), 94–112.
- Boulila, S., Haq, B.U., Hara, N., Müller, R.D., Galbrun, B., Charbonnier, G., 2021. Potential encoding of coupling between Milankovitch forcing and Earth’s interior processes in the Phanerozoic eustatic sea-level record. *Earth Sci. Rev.* 220, 103727.
- Boulila, S., Peters, S.E., Müller, R.D., Haq, B.U., Hara, N., 2023. Earth’s interior dynamics drive marine fossil diversity cycles of tens of millions of years. *Proc. Natl. Acad. Sci.* 120 (29), e2221149120.
- Cai, C., Wiens, D.A., Shen, W., Eimer, M., 2018. Water input into the Mariana subduction zone estimated from ocean-bottom seismic data. *Nature* 563, 389–392.
- Cloetingh, S., Haq, B.U., 2015. Inherited landscapes and sea level change. *Science* 347, 1258375. <https://doi.org/10.1126/science.1258375>.
- Cloetingh, S., McQueen, H., Lambeck, K., 1985. On a tectonic mechanism for regional sea-level variations. *Earth Planet. Sci. Lett.* 75 (2–3), 157–166.
- Cloetingh, S., Koptev, A., Lavecchia, A., Kovacs, I., Beekman, F., 2022. Fingerprinting secondary mantle plumes. *Earth Planet. Sci. Lett.* 597, 117819.
- Conrad, C.P., 2013. The solid Earth’s influence on sea level. *Geol. Soc. Am. Bull.* 125, 1027–1052. <https://doi.org/10.1130/B30764.1>.
- Creveling, J.R., Mitrovica, J.X., Chan, N.-H., Latychev, K., Matsuyama, I., 2012. Mechanisms for oscillatory true polar wander. *Nature* 491 (7423), 244–248.
- Davies, D.R., Valentine, A.P., Kramer, S.C., et al., 2019. Earth’s multi-scale topographic response to global mantle flow. *Nat. Geosci.* 12 (10), 845–850.
- Dawber, C.F., Tripathi, A.K., 2011. Constraints on glaciation in the middle Eocene (46–37 Ma) from Ocean Drilling Program, Site 1209 in the tropical Pacific Ocean. *Paleoceanography* 26 (2). <https://doi.org/10.1029/2010PA002037>.
- Deschamps, E., Trampert, J., 2003. Mantle tomography and its relation to temperature and composition. *Phys. Earth Planet. Inter.* 140 (4), 277–291. <https://doi.org/10.1016/j.pepi.2003.09.004>.
- Doucet, L.S., Li, Z.-X., Ernst, R.E., et al., 2019. Coupled supercontinent-mantle plume events evidenced by oceanic plume record. *Geology* 48, 159–163.
- Dutkiewicz, A., Boulila, S., Müller, R.D., 2024. Deep-sea hiatus record reveals orbital pacing by 2.4 Myr eccentricity grand cycles. *Nat. Commun.* 15 (1), 1997.
- Ernst, R.E., Bond, D.P.G., Zhang, S.-H., Buchan, K.L., Grasby, S.E., Youbi, N., El-Bilali, H., Bekker, A., Doucet, L.S., 2021. Large igneous province record through time and implications for secular environmental changes and geological time-scale boundaries. *Geophys. Monogr.* 255, 1–26.
- Exon, N.F., Haq, B.U., Von Rad, U., 1992. Exmouth Plateau revisited: scientific drilling and geological framework. *Proc. ODP Sci. Results* 122, 3–20.
- Flament, N., 2019. The deep roots of Earth’s surface. *Nat. Geosci.* 12 (10), 787–788.
- Flament, N., Gurnis, M., Müller, R.D., 2013. A review of observations and models of dynamic topography. *Lithosphere* 5, 189–210. <https://doi.org/10.1130/L245.1>.
- Francois, T., Koptev, A., Cloetingh, S., Burov, E., Gerya, T., 2018. Plume-lithosphere interactions in rifted margin tectonic settings. *Tectonophysics* 745, 138–154.
- Frizon de Lamotte, D., Fourdan, B., Leleu, S., Laparmentier, F., de Clarens, P., 2015. Style of rifting and the stages of Pangea breakup. *Tectonics* 34, 1009–1029.
- Gurnis, M., 2001. Sculpting the Earth from inside out. *Sci. Am.* 284, 40–47.
- Gurnis, M., Müller, R.D., Moresi, L., 1998. Cretaceous vertical motion of Australia and the Australian-Antarctic discordance. *Science* 279, 1499–1504.
- Haq, B.U., 1988. Geological evolution of the Indian Ocean with special reference to the Arabian Sea. In: *Marine Science of the Arabian Sea. Proceed., Internat. Conf. Am. Inst. Bio. Sci., Washington*, pp. 9–35.
- Haq, B.U., 2014. Cretaceous eustasy revisited. *Glob. Planet. Chang.* 113, 44–58. <https://doi.org/10.1016/j.gloplacha.2013.12.007>.
- Haq, B.U., 2018. Triassic eustatic variations reexamined. *Geol. Soc. Am. Today* 28 (12), 4–9.
- Haq, B.U., 2018a. Jurassic sea-level variations: a reappraisal. *Geol. Soc. Am. Today* 28 (1), 4–10.
- Haq, B.U., Huber, B.T., 2016. Anatomy of a eustatic event during the Turonian (Late Cretaceous) hot greenhouse climate. *Sci. China Earth Sci.* 60, 20–29. <https://doi.org/10.1007/s11430-016-0166-y>.
- Haq, B.U., Ogg, J.D., 2024a. Retraversing the highs and lows of Cenozoic sea level. *Geol. Soc. Am. Today*. <https://doi.org/10.1130/GSATG593A.1>.
- Haq, B.U., Ogg, J.D., 2024b. Supplemental material for retraversing the highs and lows of Cenozoic sea level. *GSA Today*. <https://doi.org/10.1130/GSAT.S25587480>.
- Haq, B.U., Schutter, S.R., 2008. A chronology of Paleozoic sea-level changes. *Science* 322, 64–68.
- Harrington, L., Zahirovic, S., Salles, T., Braz, C., Müller, R.D., 2019. Tectonic, geodynamic and surface process driving forces of Australia’s paleogeography since the Jurassic. In: Keep, M., Moss, S.J. (Eds.), *The Sedimentary Basins of Western Australia V: Proceedings of the Petroleum Exploration Society of Australia Symposium*, Perth, 29 pp.
- Hermann, J., Lakey, S., 2021. Water transfer to the deep mantle through hydrous, Al-rich silicates in subduction zones. *Geology* 49 (8), 911–915.
- Karato, S.I., Karki, B., Park, J., 2020. Deep mantle melting, global water circulation and its implications for the stability of the ocean mass. *Prog. Earth Planet. Sci.* 7, 1–25.
- Karlsen, K.S., Conrad, C.P., Magni, V., 2019. Deep water cycling and sea level change since the breakup of Pangea. *Geochim. Geophys. Geosyst.* 20, 2919–2935. <https://doi.org/10.1029/2019GC008232>.
- Karlsen, K.S., Domeier, M., Gaina, C., Conrad, C.P., 2020. A tracer-based algorithm for automatic generation of seafloor age grid from plate tectonic reconstructions. *Comput. Geosci.* 140, 104508. <https://doi.org/10.1016/j.cageo.2020.104508>.
- Kirschner, J.P., Kominz, M.A., Mwakanyamale, K.E., 2010. Quantifying extension of passive margins: implications for sea level change. *Tectonics* 29 (4).
- Kocken, J., Cramwinckel, M.J., Zeebe, R.E., Middelburg, J.J., Sluijs, A., 2019. The 405 kyr and 2.4 Myr eccentricity components in Cenozoic carbon isotope records. *Clim. Past* 15 (1), 91–104. <https://doi.org/10.5194/cp-2018-42>.
- Kocsis, A.T., Scotese, C.R., 2021. Mapping paleocoastlines and continental flooding during the Phanerozoic. *Earth Sci. Rev.* 213, 103463.
- Koppers, A.A.P., Becker, T.W., Jackson, M.C., et al., 2021. Mantle plumes and their role in Earth processes. *Nat. Rev. Earth Environ.* 2 (6), 1–20.
- Koptev, A., Cloetingh, S., 2024. Role of large igneous provinces in continental breakup, varying from “shirker” to “producer”. *Commun. Earth Environ. Sci.* 27.
- Koptev, A., Cloetingh, S., Ehlers, T.A., 2021. Longevity of small-scale (“baby”) plumes and their role in lithospheric breakup. *Geophys. J. Int.* 227 (1), 439–471.
- Korenaga, J., Planavsky, N.J., Evans, D.A., 2017. Global water cycle and the coevolution of the Earth’s interior and surface environment. *Phil. Trans. R. Soc. A* 375 (2094), 20150393.
- Kuritani, T., et al., 2019. Buoyant hydrous mantle plume from the mantle transition zone. *Sci. Rep.* 9 (1), 6549.
- Le Pichon, X., Şengör, A.M.C., Jellinek, M., Lenardic, A., İmren, C., 2023. Breakup of Pangea and the Cretaceous Revolution. *Tectonics* 42 (2), e2022TC007489.
- Liebrand, D., Beddow, H.M., Lourens, L.J., et al., 2016. Cyclostratigraphy and eccentricity tuning of the early Oligocene through early Miocene (30.1–17.1 Ma): *Cibicides mundulus* stable oxygen and carbon isotope records from Walvis Ridge Site 12. *Earth Planet. Sci. Lett.* 450, 392–405.
- Liu, Y., Huang, C., Ogg, J.G., Algeo, T.J., Kemp, D.B., Shen, W., 2019. Oscillations of global sea-level elevation during the Paleogene correspond to 1.2-Myr amplitude modulation of orbital obliquity cycles. *Earth Planet. Sci. Lett.* 522, 65–78.
- Lourens, L.J., Hilgen, F.J., 1997. Long-period variations in the Earth’s obliquity and their relation to third-order eustatic cycles and the late Neogene glaciations. *Quat. Int.* 40, 43–52.
- Magni, V., Bouilhol, P., van Hunen, J., 2014. Deep water recycling through time. *Geochim. Geophys. Geosyst.* 15, 4203–4216. <https://doi.org/10.1002/2014GC005525>.
- Marilly, C.M., Torsvik, T.H., Conrad, C.P., 2022. Global Phanerozoic sea levels from paleogeographic flooding maps. *Gondwana Res.* 110, 128–142.
- Matthews, K.J., Kara, J., Maloney, K.T., Zahirovic, S., et al., 2016. Global plate boundary evolution and kinematics since the late Paleozoic. *Glob. Planet. Chang.* 146, 226–250.
- Miller, K.G., Schmelz, W.J., Browning, J.V., Rosenthal, Y., et al., 2024. Global mean and relative sea-level changes over the past 66 Myr: implications for Early Eocene ice sheets. *Earth Sci. Syst. Soc.* 3, 10091.
- Molnar, P., England, Jones, C.H., 2015. Mantle dynamics, isostasy and the support of high terrain. *JGR Solid Earth* 120 (3), 1932–1957.
- Montelli, R., Nolet, G., Dahlen, F.A., Masters, G., 2006. A catalogue of deep mantle plumes: new results from finite-frequency tomography. *Geochim. Geophys. Geosyst.* 7 (11), 69 pp.
- Moucha, R., Forte, A.M., 2011. Changes in African topography driven by mantle convection. *Nat. Geosci.* 4, 707–712. <https://doi.org/10.1038/ngeo1235>.
- Müller, R.D., Dutkiewicz, A., 2018. Oceanic crustal carbon cycle drives 26-million-year atmospheric carbon dioxide periodicities. *Sci. Adv.* 4 (2) p.eaaq0500.

- Müller, R.D., Sdrolias, M., Gaina, C., Steinberger, B., Heine, C., 2008. Long-term sea-level fluctuations driven by ocean basin dynamics. *Science* 319 (5868), 1357–1362.
- Müller, R.D., Seton, M., Zahirovic, S., Williams, S.E., Matthews, K.J., et al., 2016. Ocean basin evolution and global-scale plate reorganization events since Pangea breakup. *Annu. Rev. Earth Planet. Sci.* 44 (1), 107–138. <https://doi.org/10.1146/annurev-earth-060115-012211>.
- Nestola, F., Smyth, J.R., 2016. Diamonds and water in the deep Earth: a new scenario. *Int. Geol. Rev.* 58 (3), 263–276.
- Pälike, H., Norris, R.D., Herrle, J.O., Wilson, P.A., Coxall, H.K., Lear, C.H., Shackleton, N. J., Tripathi, A.K., Wade, B.S., 2006. The Heartbeat of the Oligocene climate system. *Science* 314, 1894–1898.
- Parai, R.I.T.A., Mukhopadhyay, S.U.J.O.Y., 2012. How large is the subducted water flux? New constraints on mantle regassing rates. *Earth Planet. Sci. Lett.* 317, 396–406.
- Peslier, A.H., Schönbachler, M., Busemann, H., Karato, S.I., 2017. Water in the Earth's interior: distribution and origin. *Space Sci. Rev.* 212 (1–2), 743–810.
- Rampino, M.R., Caldeira, K., 2020. A 32-million year cycle detected in sea-level fluctuations over the last 545 Myr. *Geosci. Front.* 11 (6), 2061–2065.
- Rickers, F., Fichtner, A., Trampert, J., 2013. The Iceland–Jan Mayen plume system and its impact on mantle dynamics in the North Atlantic region: evidence from full-waveform inversion. *Earth Planet. Sci. Lett.* 367, 39–51.
- Sames, B., Wagreich, M., Wendler, J.E., Haq, B.U., Conrad, C.P., Melinte-Dobrinescu, M. C., et al., 2016. Short-term sea-level changes in a greenhouse world - a view from the cretaceous. *Palaeogeogr. Palaeoclimatol. Palaeoecol.* 441, 393–411.
- Schlanger, S., 1986. High frequency sea-level fluctuations in Cretaceous time: an emerging geophysical problem. *Geodyn. Ser. Am. Geophys. Union* 15, 61–74.
- Scotese, C.R., 2021. An atlas of Phanerozoic paleogeographic maps: the seas come in and the seas go out. *Annu. Rev. Earth Planet. Sci.* 49 (1), 679–728.
- Scotese, C.R., Schettino, A., 2017. Late Permian–Early Jurassic paleogeography of western Tethys and the world. In: *Permian–Triassic Salt Provinces of Europe, North Africa and the Atlantic Margins*. Elsevier, pp. 57–95.
- Simmons, M.D., Miller, K.G., Ray, D.C., et al., 2020. Phanerozoic eustasy. In: *Geologic Time Scale 2020*. Elsevier, pp. 357–400.
- Spasojević, S., Gurnis, M., 2012. Sea level and vertical motion of continents from dynamic Earth models since the Late Cretaceous. *Am. Assoc. Pet. Geol. Bull.* 96, 2037–2064.
- Stapel, G., Robinson, A., Cloetingh, S., 1996. Quantitative subsidence analysis of the Mesozoic evolution of Lusitanian Basin. *Tectonophysics* 266, 493–507.
- Stephenson, S.N., Hoggard, M.J., Holdt, M.C., White, N., 2024. Continental residual topography extracted from global analysis of crustal structure. *J. Geophys. Res. Solid Earth* 129 (4) p.e2023JB026735.
- Taylor, B., 2006. The single largest oceanic plateau: Ontong Java–Manihiki–Hikurangi. *Earth Planet. Sci. Lett.* 241 (3–4), 372–380.
- Torsvik, T.H., van der Voo, R., Preeden, U., Niocaill, C.M., Steinberger, B., Doubrovine, P.V., van Hinsbergen, D.J.J., et al., 2012. Phanerozoic polar wander, palaeogeography and dynamics. *Earth Sci. Rev.* 114 (3–4), 325–368.
- Torsvik, T.H., Domeier, M., Cocks, L.R.M., 2021. Phanerozoic paleogeography and Pangea. In: *Ancient Supercontinents and the Paleogeography of Earth*. Elsevier, pp. 577–603.
- van Dam, J.A., Aziz, H.A., Alvarez-Sierra, M.A., Hilgen, F.J., et al., 2006. Long-period astronomical forcing of mammal turnover. *Nature* 443, 687–691.
- van der Meer, D.G., van den Berg van Saparoea, A.P.H., van Hinsbergen, D.J.J., van de Weg, R.M.B., Godderis, Y., Le Hir, G., Donnadieu, Y., 2017. Reconstructing first-order changes in sea level during the Phanerozoic and Neoproterozoic using strontium isotopes. *Gondwana Res.* 44, 22–34.
- van der Meer, D.G., Scotese, C.R., Mills, B.J.W., Sluijs, A., van de Weg, R.M.B., 2022. Long-term Phanerozoic global mean sea level: insights from strontium isotope variations and estimates of continental glaciation. *Gondwana Res.* 111, 103–121.
- van Keken, P.E., Hacker, B.R., Syracuse, E.M., Abers, G.A., 2011. Subduction factory: depth-dependent flux of H₂O from subducting slabs worldwide. *J. Geophys. Res.* 116, B01401. <https://doi.org/10.1029/2010JB007922>.
- Vérard, C., 2024. On greenhouse and icehouse climate regimes over the Phanerozoic. *Terra Nova* 36, 292–297.
- Vérard, C., Hochard, C., Baumgartner, P.O., Stampfli, G.M., Liu, M., 2015. 3D Palaeogeographic reconstructions of the Phanerozoic versus sea-level and Sr-ratio variations. *J. Palaeogeogr.* 4 (1), 64–84.
- von Rad, U., Thürow, J., Haq, B.U., Gradstein, F., Ludden, J., 1989. Triassic to Cenozoic evolution of the NW Australian continental margin and the birth of the Indian Ocean (preliminary results of ODP Legs 122 and 123). *Geol. Rundsch.* 78, 1189–1210.
- von Rad, U., Exon, N.F., Haq, B.U., 1992. Rift to drift history of the Wombat Plateau NW Australia: Triassic to Tertiary, Leg 122 results. *Proc. ODP Sci. Results* 122, 765–800.
- Wade, B.S., Pälike, H., 2004. Oligocene climate dynamics. *Paleoceanography* 19, PA4019. <https://doi.org/10.1130/GSAT.52004P>.
- Wagreich, M., Lein, R., Sames, B., 2014. Eustasy, its controlling factors and the Limno-eustatic hypothesis - concepts inspired by Eduard Suess. *Aust. J. Earth Sci.* 107, 115–131.
- Wendler, J.E., Wendler, I., 2016. What drove sea-level fluctuations during the mid-Cretaceous greenhouse climate? *Palaeogeogr. Palaeoclimatol. Palaeoecol.* 441, 412–419.
- Wilson, R.C., Hiscott, R.N., Willis, M.G., Gradstein, F.M., 1989. The Lusitanian Basin of West-Central Portugal. *Am. Assoc. Pet. Geol. Mere.* 46, 341–361.
- Worsley, T.R., Nance, D., Moody, J.B., 1984. Sea level and plate dynamics. In: Haq, B.U., Milliman, J.D. (Eds.), *Marine Geology and Oceanography of Arabian Sea and Coastal Pakistan*. Van Nostrand Reinhold Co., New York, pp. 233–251.
- Wright, N.M., Seton, M., Williams, S.E., Whittaker, J.M., Müller, R.D., 2020. Sea-level fluctuations driven by changes in global ocean basin volume following supercontinent break-up. *Earth Sci. Rev.* 208, 103293.
- Xu, G., Haq, B.U., 2022. Seismic facies analysis: past, present and future. *Earth Sci. Rev.* 224, 103676.
- Young, A., Flament, N., Williams, S.E., Meredith, A., Cao, X., Müller, R.D., 2022. Long term Phanerozoic sea level change from solid Earth processes. *Earth Planet. Sci. Lett.* 584, 117451.
- Ziegler, P.A., 1989. Evolution of the North Atlantic - an overview. *Am. Assoc. Pet. Geol. Mere.* 46, 111–129.